NASA Contractor Report 179474

NASA-CR-179474
19860018995

J-Integral Estimates for Cracks in Infinite Bodies

N.E. Dowling
Virginia Polytechnic Institute and State University
Blacksburg, Virginia

July 1986

Prepared for
Lewis Research Center
Under Grant NAG 3-438

National Aeronautics and
Space Administration

J-INTEGRAL ESTIMATES FOR CRACKS IN INFINITE BODIES*

N.E. Dowling
Virginia Polytechnic Institute and State University
Department of Engineering Science and Mechanics
Blacksburg, Virginia 24061

SUMMARY

An analysis and discussion is presented of existing estimates of the J-integral for cracks in infinite bodies. Equations are presented which provide convenient estimates for Ramberg-Osgood type elasto-plastic materials containing cracks and subjected to multiaxial loading. The relationship between J and the strain normal to the crack is noted to be only weakly dependent on state of stress. But the relationship between J and the stress normal to the crack is strongly dependent on state of stress. A plastic zone correction term often employed is found to be arbitrary, and its magnitude is seldom significant.

*Material also submitted to Engineering Fracture Mechanics for publication.

CONTENTS

INTRODUCTION

Materials are considered which have a uniaxial stress-strain relationship of the form:

$$\varepsilon/\varepsilon_o = \sigma/\sigma_o + \alpha(\sigma/\sigma_o)^n \qquad (1)$$

where σ is stress, σ_o, ε_o, and α are constants more fully explained later, and n is a constant generally called the strain hardening exponent. The first and second terms represent, respectively, elastic and plastic components of the total strain, ε.

Configurations of cracks in infinite bodies which are of interest are shown in Fig. 1. Two dimensional cases as in Fig. 1a may be either plane stress or plane strain, depending on the situation in direction 3. Note that a stress, S, is applied remote from the crack in a direction normal to the plane of the crack. Remotely applied transverse stresses, T, are also considered. Figure 1b illustrates remotely applied axisymmetric loading of a circular crack. The stress normal to the plane of the crack is again S, and T is the stress in all radial directions in the plane of the crack. Edge or surface crack configurations correspond to bisecting either Fig. 1a or 1b along the 1-3 plane.

Some early work related to this discussion is that of Shih [1] and Shih and Hutchinson [2], which established the general form of estimates of J for cracked members of Eq. 1 type material. The EPRI Elastic-Plastic Fracture Analysis handbook [3] later pursued such estimates in considerable detail, but only for cracks in finite bodies. He and Hutchinson [4,5] have reported analytical results for infinite body cases as in Fig. 1 that figure prominantly in what follows. They

considered multiaxial loading (various ratios T/S) and remote strains that are predominantly plastic, so that Eq. 1 reduces to:

$$\varepsilon/\varepsilon_o = \alpha(\sigma/\sigma_o)^n \qquad (2)$$

Numerical results for certain cases of uniaxial loading (T = 0) are also reported by Trantina et. al. [6,7] using Eq. 1. In addition, Wilson [8] has previously studied two-dimensional cases of uniaxial loading, considering not only Eq. 1 but also bilinear and piecewise power hardening. Also, I previously presented limited discussion of this subject in Appendices to two papers [9,10] that included use of such J-integral estimates in analyzing growth data for small fatigue cracks.

It is the purpose of this paper to provide a useful analysis and discussion of J-integral estimates for cracks in infinite bodies of Eq. 1 type materials. The estimates are reduced to a convenient form for application to engineering or research problems. Also, discussion is presented concerning certain important aspects of the estimates, including multiaxial effects, and a plastic zone correction term.

STRESS-STRAIN RELATIONSHIPS

Before proceeding, it is useful to further explain the uniaxial stress-strain relationship, Eq. 1, and also to extend this to cases of multiaxial loading.

Uniaxial Stress-Strain Curve

Figure 2 illustrates a curve corresponding to Eq. 1. The curve gradually diverges from an elastic line having a slope:

$$E = \sigma_o/\varepsilon_o \tag{3}$$

Hence, $(\varepsilon_o, \sigma_o)$ is a point on the elastic line, not on the actual curve. The constant σ_o may be thought of as a yield strength defined in the conventional manner by a plastic strain offset. Then $(\varepsilon_y, \sigma_o)$ is a point on the actual curve, where

$$\varepsilon_y = (1 + \alpha)\varepsilon_o \tag{4}$$

And the plastic strain offset is:

$$\varepsilon_{py} = \alpha\ \varepsilon_o$$

Of the three constants ε_o, σ_o, and α, any one of them may be arbitrarily chosen, and then the other two fitted to the particular curve of interest. For a given set of values of these constants, there is a family of curves, all passing through the point $(\varepsilon_y, \sigma_o)$, and each corresponding to a different value of n. Hence, the value of n also needs to be fitted to the particular curve of interest.

Of the three constants ε_o, σ_o, and α, the latter is the most logical to be arbitrarily chosen. The constant α can be thought of as representing the relative magnitude of the plastic strain offset.

$$\alpha = \varepsilon_{py}/\varepsilon_o = \varepsilon_{py} E/\sigma_o \tag{5}$$

Conventional plastic strain offsets, such as $\varepsilon_{py} = 0.002$ for engineering metals, generally correspond to α in the range 0.1 to 1.0.

Multiaxial Stress-Strain Relationships

All of the equations to be used later involve only the stresses and strains remote from the crack. No remote shear stresses are applied and the material is assumed to be isotropic, so that the axes shown in Fig. 1 are also the principal axes for both stress and strain. These principal stresses and strains will be denoted by σ_i and ε_i, where i corresponds to any one of the directions in Fig. 1. Subscripts j and k then indicate the remaining two directions.

Strains may be separated into elastic and plastic components.

$$\varepsilon_i = \varepsilon_{ei} + \varepsilon_{pi} \tag{6}$$

where the subscripts e and p indicate these components. The stresses and the elastic strains are related by Hooke's law.

$$\varepsilon_{ei} = \frac{1}{E} [\sigma_i - \nu (\sigma_j + \sigma_k)] \tag{7}$$

where ν is the elastic constant, Poisson's ratio. (A value of $\nu = 0.3$ is used throughout this paper as being typical for engineering metals).

As only constant ratios T/S are considered, proportional remote loading applies, and a total deformation plasticity theory can be used for the remote stresses and strains. In this context, stresses and plastic strains are related by:

$$\varepsilon_{pi} = \frac{1}{E_p} [\sigma_i - 0.5 (\sigma_j + \sigma_k)] \tag{8}$$

where

$$E_p = \bar{\sigma}/\bar{\varepsilon}_p \tag{9}$$

The quantity $\bar{\sigma}$ is the effective stress

$$\bar{\sigma} = \left[\frac{(\sigma_1 - \sigma_2)^2 + (\sigma_2 - \sigma_3)^2 + (\sigma_3 - \sigma_1)^2}{2}\right]^{1/2} \tag{10}$$

and $\bar{\varepsilon}_p$ is the effective plastic strain

$$\bar{\varepsilon}_p = \left[\frac{2}{3}\left(\varepsilon_{p1}^2 + \varepsilon_{p2}^2 + \varepsilon_{p3}^2\right)\right]^{1/2} \tag{11}$$

Substituting Eqs. 7 and 8 into Eq. 6 gives the following relationship between stresses and total strains:

$$\varepsilon_i = \frac{1}{E_t}\left[\sigma_i - \tilde{\nu}\left(\sigma_j + \sigma_k\right)\right] \tag{12}$$

where

$$E_t = \bar{\sigma}/\bar{\varepsilon} \tag{13}$$

The quantity $\bar{\varepsilon}$ is the effective total strain, given by:

$$\bar{\varepsilon} = \bar{\sigma}/E + \bar{\varepsilon}_p \tag{14}$$

and $\tilde{\nu}$ is an effective Poisson's ratio.

$$\tilde{\nu} = \frac{\nu\bar{\sigma} + 0.5\, E\bar{\varepsilon}_p}{E\bar{\varepsilon}} \tag{15}$$

Note that as $\bar{\varepsilon}$ is increased from predominantly elastic to predominantly plastic strain, $\tilde{\nu}$ increase smoothly from ν to 0.5, so that Eq. 12 reduces to Eq. 7 in the former case, and to Eq. 8 in the latter case. Also, substituting the inverse of the three equations represented by Eq. 12 into Eq. 10 gives an expression for $\bar{\varepsilon}$ as a function of the principal total strains:

$$\bar{\varepsilon} = \frac{1}{1 + \tilde{\nu}} \left[\frac{(\varepsilon_1 - \varepsilon_2)^2 + (\varepsilon_2 - \varepsilon_3)^2 + (\varepsilon_3 - \varepsilon_1)^2}{2}\right]^{1/2} \tag{16}$$

For predominately plastic strains, where $\tilde{\nu} = 0.5$, Eq. 16 reduces to Eq. 11. And for predominately elastic strain, where $\tilde{\nu} = \nu$, substitution of Eq. 7 into Eq. 16 gives Eq. 10.

Effective stresses and plastic and total strains as defined above coincide with the corresponding quantities for the uniaxial case, so that Eq. 1 can be generalized to:

$$\bar{\varepsilon}/\varepsilon_o = \bar{\sigma}/\sigma_o + \alpha\,(\bar{\sigma}/\sigma_o)^n \tag{17}$$

Hence, the constants ε_o, σ_o, α, and n for use in Eq. 17 can be evaluated from a uniaxial stress-strain curve.

For the particular cases of interest of Fig. 1, Eqs. 10 and 12 may be used to derive ratios between the effective stresses and strains and the corresponding stresses and strains in the direction normal to the plane of the crack. These ratios, which will be needed later, are given below. The loading in the plane of the crack is characterized in terms of the quantity R.

$$R = T/S \tag{18}$$

(a) Plane stress: $\sigma_1 = S,\ \sigma_2 = T,\ \sigma_3 = 0$

$$\bar{\sigma}/S = \sqrt{1 - R + R^2} \tag{19a}$$

$$\bar{\varepsilon}/\varepsilon_1 = \frac{\bar{\sigma}/S}{1 - \tilde{\nu}R} \tag{19b}$$

(b) Plane strain: $\sigma_1 = S,\ \sigma_2 = T,\ \varepsilon_3 = 0$

$$\bar{\sigma}/S = \sqrt{(1 + R)^2\,(1 - \tilde{\nu} + \tilde{\nu}^2) - 3R} \tag{20a}$$

$$\bar{\varepsilon}/\varepsilon_1 = \frac{\bar{\sigma}/S}{1 - \tilde{\nu}^2 - \tilde{\nu}R\ (1 + \tilde{\nu})} \tag{20b}$$

(c) Axisymmetric case: $\sigma_1 = S,\ \sigma_2 = \sigma_3 = T$

$$\bar{\sigma}/S = \left|1 - R\right| \tag{21a}$$

$$\bar{\varepsilon}/\varepsilon_1 = \frac{\bar{\sigma}/S}{1 - 2\tilde{\nu}R} \tag{21b}$$

RESULTS OF HE AND HUTCHINSON FOR ELASTIC STRAINS SMALL

In the work of He and Hutchinson (4,5) numerical results for the J-integral, J_p, for Eq. 2 type material are presented by tabulating values of $h_1 = h_1(n,R)$,

where

$$h_1(n,R) = \frac{J_p}{\bar{\sigma}\bar{\varepsilon}a} \tag{22}$$

Various combinations of n and R = T/S were investigated for the configurations of Fig. 1.

In addition, a perturbation approach was used [4,5] to obtain closed form estimates for the plane strain and axisymmetric cases. These are as follows, with the obvious guess for plane stress also being included:

(a) Plane stress:

$$\frac{J_p}{\bar{\sigma}\bar{\varepsilon}a} = h_1' = \pi\sqrt{n}\left(\frac{f_1 S}{\bar{\sigma}}\right)^2 \tag{23}$$

(b) Plane strain:

$$\frac{J_p}{\bar{\sigma}\bar{\varepsilon}a} = h_1' = \frac{3\pi\sqrt{n}}{4}\left(\frac{f_1 S}{\bar{\sigma}}\right)^2 \tag{24}$$

(c) Axisymmetric:

$$\frac{J_p}{\bar{\sigma}\bar{\varepsilon}a} = h_1' = \frac{6}{\pi\sqrt{1 + 3/n}}\left(\frac{f_1 S}{\bar{\sigma}}\right)^2 \tag{25}$$

The factor $f_1 = 1$ for central or interior cracks as in Fig. 1. It is introduced so that cases of edge or surface cracks are included, with these being described by bisecting Fig. 1a or b along the 1-3 plane. Values of f_1 will be estimated from the linear elastic case (n = 1), for

example, $f_1 = 1.12$ for two dimensional edge cracks formed by bisecting Fig. 1a.

Figures 3-6 compare each numerical result from refs. 4 and 5 with the closed form estimate from one of Eqs. 23-25. Ratios of the estimated value h_1' to the numerical result h_1 are plotted for each value of the strain hardening exponent, n, where there is a numerical result. The numerical h_1 values are either upper or lower bounds, with both bounds being available in only a few cases. Arrows are therefore shown in Figs. 3-6 to indicate that the true ratio h_1'/h_1 may be above or below the value plotted, as appropriate in each case.

Figure 3 gives the comparisons for central cracks under plane strain, where there are numerical results for T/S = 0, -1, and 0.5. Figure 4 gives comparisons for edge cracks under plane strain, and for central and edge cracks under plane stress, for which cases numerical results are available for T/S = 0 only. The ratio h_1'/h for these cases deviates increasingly from unity as n is increased up to the highest value used of 7. Most of the values are within 10% of unity, and all are within 16%.

Note that both bounds are available for central and edge cracks under plane strain with T/S = 0. Here, h_1'/h_1 for the middle of the bounds is below but within 5% of unity for central cracks, and above but within 11% of unity for edge cracks. As pointed out in Ref. 5, this implies that f_1 is actually not constant at the value of 1.12, but decreases with n, perhaps approaching unity for large n.

Figures 5 and 6 give h_1'/h_1 ratios for the wide range of T/S values studied for the axisymmetric case. Lower bounds only are available from

Ref. 4 for n up to 10, and also for $n = \infty$. The figures show all but the $n = \infty$ results, which are as follows:

T/S	0	-1	-4	-9	.5	.67	.75
h_1'/h_1	1.037	1.073	1.087	1.093	1.146	0.942	0.549

For $T/S \leq 0$, the ratio h_1'/h_1 is within 10% of unity for all n values. But for $T/S > 0$, the discrepancy is almost 50% for the combinations of large n and high T/S value.

If it is assumed that the numerical bounds on h_1 for the various cases of Figs. 3-6 are reasonably close to the actual values, say within 10%, then the simple estimates from Eqs. 23-25 are suitable for most purposes. Note that the only large discrepancies occur for axisymmetric cases approaching triaxial tension (T/S = 1), which state of stress is rare in practical applications. Caution is obviously needed for large n values, and additional numerical results are needed to confirm or modify this tentative conclusion.

ESTIMATES FOR ELASTO-PLASTIC MATERIALS

Based on the work of Shih (1) and Shih and Hutchinson (2), J-integral values for Eq. 1 type materials may be estimated as follows:

$$J = J_e + J_z + J_p \tag{26}$$

where J_p is the estimate of J for Eq. 2 type material which has a stress versus strain curve that is the same as the stress versus plastic strain curve for the Eq. 1 type material of interest. (This would be satisfied if the constants ε_o, σ_o, α, and n are the same.)

The term J_e is calculated for a linear-elastic material with the same elastic modulus, $E = \sigma_o/\varepsilon_o$, as the Eq. 1 type material.

$$J_e = \frac{K^2}{E'} = \frac{C_o \pi S^2 a}{E'} \tag{27}$$

where

$E' = E$ (plane stress)

$E' = E/(1 - \nu^2)$ (plane strain, and axisymmetric)

The quantity K is the Mode I stress intensity factor of linear elastic fracture mechanics, which is given by:

$$K = f_1 f_2 S\sqrt{\pi a} \tag{28}$$

Note that the geometry factor is separated into the product of a free surface correction factor, f_1, as in Eqs. 23-25, and a residual geometry factor, f_2, with values as follows:

Case	f_1	f_2	C_o
Fig. 1a - Central crack, plane stress or plane strain	1.0	1.0	1.0
Bisected Fig. 1a - Edge crack, plane stress or plane strain	1.12	1.0	1.25
Fig. 1b - Internal circular crack	1.0	$2/\pi$	0.405
Bisected Fig. 1b - Half-circular surface crack	1.035	$2/\pi$	0.434

From comparison of Eqs. 27 and 28, note that:

$$C_o = f_1^2 \, f_2^2 \tag{29}$$

The values of f_1 and f_2 are the well known values available from any good collection of linear-elastic fracture mechanics results, such as Ref. 11. As shown in Ref. 6 and previously elsewhere, f_1 for a half-circular surface crack varies around the periphery of the crack, decreasing from about 1.2 at the intersection with the free surface to about 1.035 at the point of maximum depth.

Note that J cannot be separated into elastic and plastic terms, J_e and J_p, in a formal mathematical sense. This summation as in Eq. 26 is only a strategy adopted to obtain an estimate. It provides correct values at the limiting case of linear-elastic loading, that is, negligible plastic strain, where $J = J_e$, and also at the limiting case of large plastic strain, that is, negligible elastic strain, where $J = J_p$.

The term J_z of Eq. 26 is based on a plastic zone calculation and is used in Refs. 1 and 2 to smooth the transition between the limiting cases. Following Ref. 3, the linear-elastic solution, Eq. 27, is

modified by replacing the crack dimension "a" with an effective value, a_e.

$$a_e = a + \Phi r_y \tag{30}$$

where

$$r_y = \frac{1}{C_2 \pi} \left(\frac{n-1}{n+1}\right) \left(\frac{K}{\sigma_o}\right)^2 \tag{31a}$$

$$C_2 = 2 \qquad \text{(plane strain)} \tag{31b}$$

$$C_2 = 6 \qquad \text{(plane strain, and axisymmetric)} \tag{31c}$$

$$\Phi = \frac{1}{1 + (P/P_o)^2} \tag{31d}$$

The quantity P/P_o is the ratio of the applied load to a limit or reference load based on the stress σ_o. For cases of cracks in infinite bodies, and considering multiaxial loading, the following substitution is appropriate:

$$P/P_o = \bar{\sigma}/\sigma_o \tag{32}$$

The modified value of J_e is:

$$J_e' = J_e \frac{a + \Phi r_y}{a} \tag{33}$$

and the increase of J_e' over J_e is defined as J_z .

$$J_z = J_e' - J_e = \frac{\Phi r_y}{a} J_e \tag{34}$$

Combining Eqs. 28, 29, 31 and 34 gives:

$$\frac{J_z}{J_e} = \frac{C_o}{C_2} \left(\frac{n-1}{n+1}\right) \left(\frac{S}{\bar{\sigma}}\right)^2 \frac{(\bar{\sigma}/\sigma_o)^2}{1 + (\bar{\sigma}/\sigma_o)^2} \tag{35}$$

It is convenient to normalize the estimated J from Eq. 26 to the elastic term.

$$J/J_e = 1 + J_z/J_e + J_p/J_e \tag{36}$$

Only J_p/J_e remains to be evaluated. This is obtained by noting that the effective plastic strain is given by the second term of Eq. 17.

$$\bar{\varepsilon}_p/\varepsilon_o = \alpha(\bar{\sigma}/\sigma_o)^n \tag{37}$$

Also, $\bar{\varepsilon}$ in Eq. 22 must be interpreted as equal to this $\bar{\varepsilon}_p$, as J_p is estimated for an Eq. 2 type material with negligible elastic strain. Then combining Eqs. 22, 27, 36, and 37 leads to:

$$\frac{J}{J_e} = 1 + \frac{J_z}{J_e} + \frac{h_1 \alpha E'}{C_o \pi E} \left(\frac{\bar{\sigma}}{S}\right)^2 \left(\frac{\bar{\sigma}}{\sigma_o}\right)^{n-1} \tag{38}$$

Recall that $\bar{\sigma}/S$ is given by the appropriate one of Eqs. 19-21. The combination of Eqs. 35 and 38, when reduced to the limiting case of uniaxial loading (T/S = 0), is similar to Eq. 18 of the paper by Wilson (8).

A simplified version of Eq. 38 which employs the estimates of h_1 from Eqs. 23-25 is as follows:

$$\frac{J}{J_e} = 1 + \frac{J_z}{J_e} + h_o \frac{E'}{E} \frac{\bar{\varepsilon}_p}{\bar{\varepsilon}_e} \tag{39}$$

where, consistent with Eq. 14:

$$\bar{\varepsilon}_e = \bar{\sigma}/E \tag{40}$$

And the expressions for h_o are:

$$h_o = \sqrt{n} \qquad \text{(plane stress)} \tag{41a}$$

$$h_o = \frac{3\sqrt{\bar{n}}}{4} \qquad \text{(plane strain)} \qquad (41b)$$

$$h_o = \frac{3}{2\sqrt{1 + 3/n}} \qquad \text{(axisymmetric)} \qquad (41c)$$

In addition, it will be shown below that J_z/J_e is often small, so that reasonable estimates are given by:

$$\frac{J}{J_e} = 1 + h_o \frac{E'}{E} \frac{\bar{\varepsilon}_p}{\bar{\varepsilon}_e} \qquad (42)$$

It is sometimes convenient to employ an equivalent K value which is modified from the elastic value based on the J-integral. Using Eqs. 27 and 42 gives:

$$K_{eq} = \sqrt{JE'} = K\left(1 + h_o \frac{E'}{E} \frac{\bar{\varepsilon}_p}{\bar{\varepsilon}_e}\right)^{1/2} \qquad (43)$$

Hence, from Eqs. 42 and 43, a correction factor can be applied to a J_e or K value for the linear-elastic case, with this factor depending on the strain hardening exponent through h_o and the relative degree of plasticity, as expressed by the ratio of the effective plastic to effective elastic strain.

DISCUSSION

Discussion follows under three subheadings. First, there is a discussion of the trends in J-integral values with state of stress. Next, there are comparisons with existing analytical results for elasto-plastic materials. Finally, the plastic zone correction term is discussed.

State of Stress Trends

A question of some importance is whether the J-integral has the potential of predicting fracture and fatigue of real materials where multiaxial loading affects the behavior (12). First, note that the elastic term, Eq. 27, is not affected by the in-plane stress, T, as it depends only on S. The plastic zone term, Eq. 35, is affected by T, but this is unimportant, as this term is seldom a significant fraction of the total J value. But the plastic term, such as the last term of Eq. 38 or 39, is strongly affected by T. This occurs as a result of the effective stress and strain quantities which appear.

Figures 7 and 8 illustrate the trends for the axisymmetric case for various ratios of the stresses T/S. Figure 7 plots J versus the principal strain in the direction normal to the crack, and Fig. 8 plots J versus the principal stress, $\sigma_1 = S$, in this same direction. These curves are based on typical values of $n = 7$ and $\nu = 0.3$, a value of $\alpha = 1$ is arbitrarily chosen, and the plots apply for any choice of σ_o and ε_o. The approximate form represented by Eqs. 39 and 41c is used, except that Eq. 38 with an interpolated numerical h_1 value is used at $T/S = 0.75$. This is done as the approximation is less than about 5% except for $T/S = 0.75$, where it would have been about 25%. Note that

Eqs. 21a and b were also employed in the calculations to obtain these curves.

It is interesting that J is only weakly affected by state of stress when comparisons are made based on principal strain, but drastically affected for comparisons based on principal stress. In addition, the trend of higher J values for lower T/S values is at least qualitatively consistent with the empirical trends observed in fracture and fatigue response of materials.

Consider a given material and a given choice among plane stress, plane strain, or the axisymmetric case. Equation 38 then gives a nearly unique relationship between J and either effective stress, $\bar{\sigma}$, or effective strain, $\bar{\varepsilon}$, which is independent of the stress ratio T/S. Furthermore, if the approximations of Eq. 41 are used, and if the plastic zone term is omitted by the use of Eq. 42, the relationships between J and $\bar{\varepsilon}$, and between J and $\bar{\sigma}$, are exactly unique.

Comparisons With Elasto-Plastic Analysis of Trantina

References 6 and 7 present J-integral results from finite element analysis using an elasto-plastic stress-strain curve of the form of Eq. 1. The approximation involved in summing separately computed elastic and plastic terms to obtain J is not necessary. Hence, these results provide a valuable comparison with the estimates presented above.

All of the analysis in Refs. 6 and 7 is for uniaxial loading. Reference 6 considers the important three-dimensional case of a half-circular surface crack, and Ref. 7 considers circumferential cracks growing from spherical and other voids. Figures 9 and 10 compare these analytical results with estimates from Eqs. 35 and 39. The various constants used in the estimates are as follows:

	Fig. 9 estimates based on: circular crack	Fig. 9 estimates based on: 2D crack	Fig. 10 estimates (circular crack)
C_o	0.434	0.434	0.405
C_2	6	6	6
E'/E	$1/(1-\nu^2)$	$1/(1-\nu^2)$	$1/(1-\nu^2)$
h_o	$3/2\sqrt{1 + 3/n}$	$3\sqrt{n}/4$	$3/2\sqrt{1 + 3/n}$

For a half-circular surface crack, estimates made based on h_o for a circular crack give curve 1 in Fig. 9, which falls considerably below the analytical results. Note that this case is a complex three dimensional one, and the special situation existing for a circular crack under axisymmetric loading may not exist even approximately. The possibility exists that the behavior is closer to that for a two-dimensional crack. Hence, an alternate estimate is made which is the same except that h_o is taken from Eq. 41b, which applies for two-dimensional cracks in plane strain. This yields curve 2 in Fig. 9, which is in excellent agreement with the analysis.

Note that the comparisons with the analysis of Ref. 6 depend on the position around the periphery of the crack. The above comparisons are all for the point of maximum depth, and the appropriate value of $f_1 = 1.035$ is used in normalizing the values from Ref. 6 to obtain J/J_e for plotting in Fig. 9.

Reference 6 also contains limited analysis for $n = 20$. Similar comparisons were made, and similar results were obtained. In particular, h_o for circular cracks (Eq. 41c) gives estimates which are low by more than a factor of 2 at $\varepsilon/\varepsilon_o = 1.35$. But use of h_o for two-dimensional plane strain (Eq. 41b) gives an estimate which is high by

only 8% at $\varepsilon/\varepsilon_0 = 1.35$.

Figure 10 gives comparisons of analysis and estimates for a circumferential crack at a spherical void. The estimates are based on the assumption that this geometry is equivalent to a circular crack of radius $a = R + \ell$, where R and ℓ are defined in Fig. 10. In other words, the crack tip is assumed to be sufficiently remote that there is no effect of the local stress concentration of the spherical void.

Figure 10 shows reasonable agreement between estimates and analysis for n = 5, 10 and 20. The J values from analysis at the higher strains are 10 to 20% higher than the estimates. Note that, for linear elasticity (n = 1), the effect at $\ell/R = 0.5$ of the stress concentration of the spherical void is to elevate the value of f_2 by a factor [13] of about 1.04, where the interpretation $a = R + \ell$ is made for Eq. 27, so that:

$$C_0 = (1.04 \times 2/\pi)^2 = 0.438$$

Since this new value of C_0 is used in normalizing the analytical results of Ref. 7 to obtain J/J_e, the effect of the stress concentration has been removed from the comparisons to this extent. The fact that the analytical values are still higher than the estimates may indicate that the effect of the stress concentration on J/J_e is greater for the higher n values.

In preparing Fig. 10, it was necessary to know the ε_0 value used in Ref. 7. This value is $\varepsilon_0 = 0.005776$ and was obtained from information kindly provided to the author by Trantina.

Note that the approximation using a simple circular crack of radius $a = R + \ell$ is the long crack limiting case for the actual problem of a circumferential crack at a spherical void. For linear-elasticity, the

difference between this case and the actual solution becomes significant, say > 20% in K, around $\ell/R = 0.08$. For small ℓ/R, the actual solution deviates drastically from the long crack limiting case and becomes dominated by the local stress field of the spherical void [13,14]. Similar behavior is expected for $n > 1$, so that estimates similar to those just described could not be reasonably applied to the analysis of Ref. 7 for $\ell/R = 0.1$.

To summarize, the comparisons of Figs. 9 and 10 provide encouragement that the proposed estimates are reasonable. However, no analytical results for an Eq. 1 type material appear to be available which allow the inaccuracies of the estimates to be isolated. The Fig. 9 comparison is complicated by the three-dimensional nature of the half-circular surface crack, and the Fig. 10 comparison is complicated by the spherical void.

Plastic Zone Correction Term

In the estimates of J for an Eq. 1 type material provided by Eq. 38 or 39, the elastic (first) term dominates at low strain, and the plastic (third) term dominates at high strain. The plastic zone (second) term makes its greatest relative contribution at intermediate values of strain. This is illustrated by Fig. 11, where J_z/J computed from Eqs. 35 and 39 is plotted versus strain for an interior crack under plane strain with $T/S = 0$. A typical value of $n = 7$ is chosen, and four different α values are employed. The strains plotted are normalized to a common value of yield strain rather than the individual ε_0 values corresponding to each α. This common yield strain was chosen as the ε_y value from Eq. 4 corresponding to $\alpha = 1$, called ε_y'. Strains

normalized to this value are calculated from strains normalized to ε_o by noting that:

$$\varepsilon_y' = \varepsilon_o(1 + \alpha')\ (\alpha'/\alpha)^{1/(n-1)}$$

where $\alpha'=1$ is the chosen standard value.

Two significant facts are observed from Fig. 11. First, the plastic zone correction term has the undesirable property of depending on the arbitrary coice of α. And second, for any reasonable choice of α, typically 0.1 to 1, the J_z term is never a significant fraction of the total J. For the case of Fig. 11, the J_z term is always less than 10% of J, even for the extreme choice of $\alpha = 0.01$.

The dependence on α arises from the fact that, for a given stress-strain curve, different choices of α result in different values of σ_o. The size of the estimated plastic zone decreases if σ_o is increased, which corresponds to increased α, with the result that J_z/J_e decreases. This can be seen by studying Eqs. 3-5 and 35.

Plots similar to Fig. 11 were made for a wide variety of cases, and the peak J_z/J values were noted for each case. The approximate estimates employing h_o in Eq. 39 were used, except that Eq. 38 with the numerical h_1 value was used where this was known to gave a difference in the plastic (third) term exceeding 15%. Figure 12 summarizes the peak effect of the plastic zone correction as a function of n for uniaxial loading for both $\alpha = 0.1$ and 1. The largest effect is for plane stress, and this never exceeds 15% for n up to 10.

Figure 13 shows the effect of various degrees of in-plane loading on the axisymmetric case for n values up to 10. The plastic zone term is most significant for states of stress approching hydrostatic tension,

approaching 30% for T/S = 0.75 and n = 10. For plane stress and plane strain with n up to 10 and T/S up to 0.75, the estimated value of J_z/J seldom exceeds 10%. The exceptions are plane stress at T/S = 0, as shown in Fig. 12, and plane strain at T/S = 0.75, where J_z/J_e is around 20%.

Accurate numerical analysis for Eq. 1 type material would be needed for critical cases where J_z/J is large to determine if the J_z/J correction term is necessary and to guide in the choice of α. However, at present it appears that the term is generally unnecessary, in addition to being arbitrary due to the effect of α.

CONCLUDING REMARKS

Estimates of J from the relatively simple Eq. 42 appear to be suitable for most practical purposes. More specific estimates (Eq. 38) may be needed for axisymmetric loading which approaches triaxial tension. For nonaxisymmetric cases, such as two-dimensional plane stress and plane strain, caution is needed for high tension loads in the plane of the crack, and for large values of the strain hardening exponent, n, where analytical support for Eq. 42 is weak.

The dependence of the plastic term of the J estimates on the ratio of effective plastic strain to effective elastic strain is significant. This corresponds to a dependence of J on state of stress which is quite large for a given value of stress normal to the crack.

Additional work is needed on the complex three-dimensional, but practically important, case of a half-circular surface crack. Preliminary indications are that the J values exceed estimates based on the axisymmetric case.

The plastic zone correction term is both small and arbitrary. It should be neglected until additional analysis establishes its need and removes its arbitrariness.

REFERENCES

1. Shih, C. F., "J-Integral Estimates for Strain Hardening Materials in Antiplane Shear Using Fully Plastic Solutions," Mechanics of Crack Growth, ASTM STP 590, 1976, pp. 3-26.

2. Shih, C. F., and Hutchinson, J. W., "Fully Plastic Solutions and Large Scale Yielding Estimates for Plane Stress Crack Problems," Jnl. of Engineering Materials and Technology, ASME, Vol. 98, No. 4, Oct. 1976, pp. 289-295.

3. Kumar, V., German, M. D., and Shih, C. F., "An Engineering Approach for Elastic-Plastic Fracture Analysis," EPRI NP-1931, Project 1237-1, Electric Power Research Institute, Palo Alto, Cal., July 1981.

4. He, M. Y., and Hutchinson, J. W., "The Penny Shaped Crack and the Plane Strain Crack in an Infinite Body of Power-Law Material," Jnl. of Applied Mechanics, ASME, Vol. 48, No. 4, Dec. 1981, pp. 830-840.

5. He, M. Y., and Hutchinson, J. W., "Bounds for Fully Plastic Crack Problems for Infinite Bodies," Elastic-Plastic Fracture: Second Symposium, Vol. 1, ASTM STP 803, American Society for Testing and Materials, 1983, pp. 277-290.

6. Trantina, G. G., deLorenzi, H. G., and Wilkening, W. W., "Three-Dimensional Elastic-Plastic Finite Element Analysis of Small Surface Cracks," Engineering Fracture Mechanics, Vol. 18, No. 5, 1983, pp. 925-938.

7. Trantina, G. G., and Barishpolsky, M., "Elastic-Plastic Analysis of Small Defects - Voids and Inclusions," Engineering Fracture Mechanics, Vo. 20, No. 1, 1984, pp. 1-10.

8. Wilson, W. K., "J-Integral Estimates for Small Edge and Interior Cracks," Engineering Fracture Mechanics, Vol. 20, No. 4, 1984, pp. 655-665.

9. Dowling, N. E., "Crack Growth During Low-Cycle Fatigue of Smooth Axial Specimens," Cyclic Stress-Strain and Plastic Deformation Aspects of Fatigue Crack Growth, ASTM STP 637, 1977, pp. 97-121.

10. Dowling, N. E., "Growth of Small Fatigue Cracks in an Alloy Steel," Paper No. 83-PVP-94, ASME 4th National Congress on Pressure Vessel and Piping Technology, June 19-24, 1983, Portland, Oregon.

11. Tada, H., Paris, P. C., and Irwin, G. R., The Stress Analysis of Cracks Handbook, Del Research Corp., Hellertown, Pa., 1973.

12. Miller, K. J., and Kfouri, A. P., "A Comparison of Elastic-Plastic Fracture Parameters in Biaxial Stress States," Elastic-Plastic Fracture, ASTM STP 668, American Society for Testing and Materials, 1979, pp. 214-228.

13. Baratta, F. I., "Refinements of Stress Intensity Factor Estimates for a Peripherally Cracked Spherical Void and a Hemispherical Surface Pit," Jnl. of the American Ceramic Society - Communications, Vol. 64, No. 1, 1981, pp. C3-C4.

14. Dowling, N. E., "Fatigue at Notches and the Local Strain and Fracture Mechanics Approaches," Fracture Mechanics, ASTM STP 677, 1979, pp. 247-273.

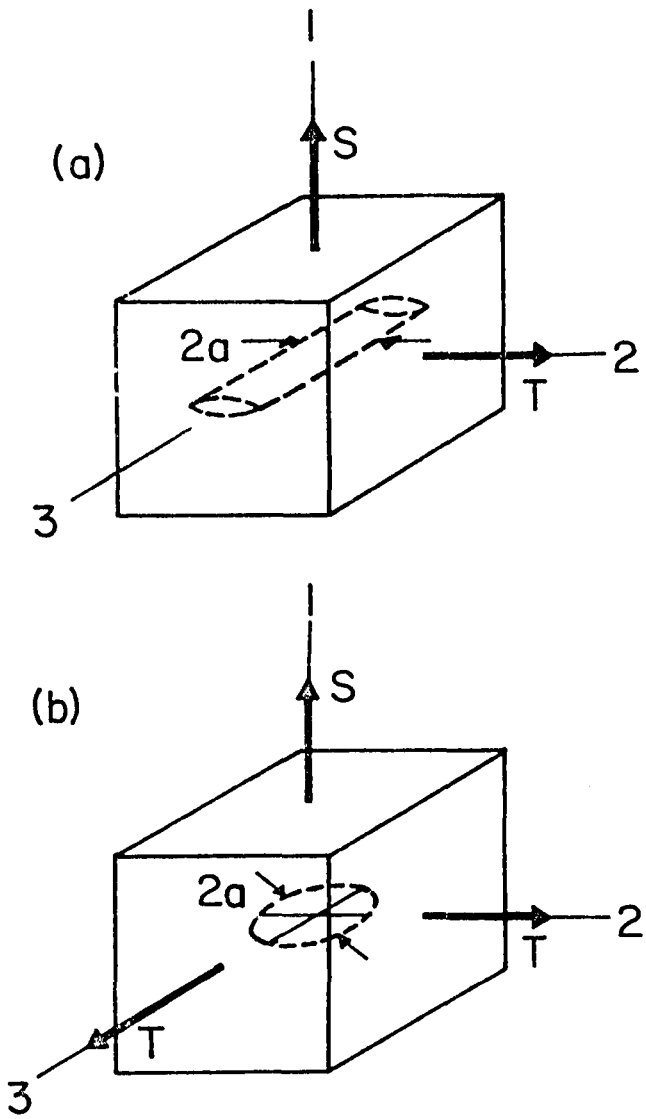

Fig. 1 - Cracked body configurations considered: (a) Two dimensional cases, either plane stress ($\sigma_3 = 0$) or plane strain ($\varepsilon_3 = 0$). (b) Circular crack under axisymmetric loading. Bisecting (a) along the 1-3 plane describes cases of two dimensional edge cracks, and bisecting (b) along the 1-3 plane gives a half-circular surface crack.

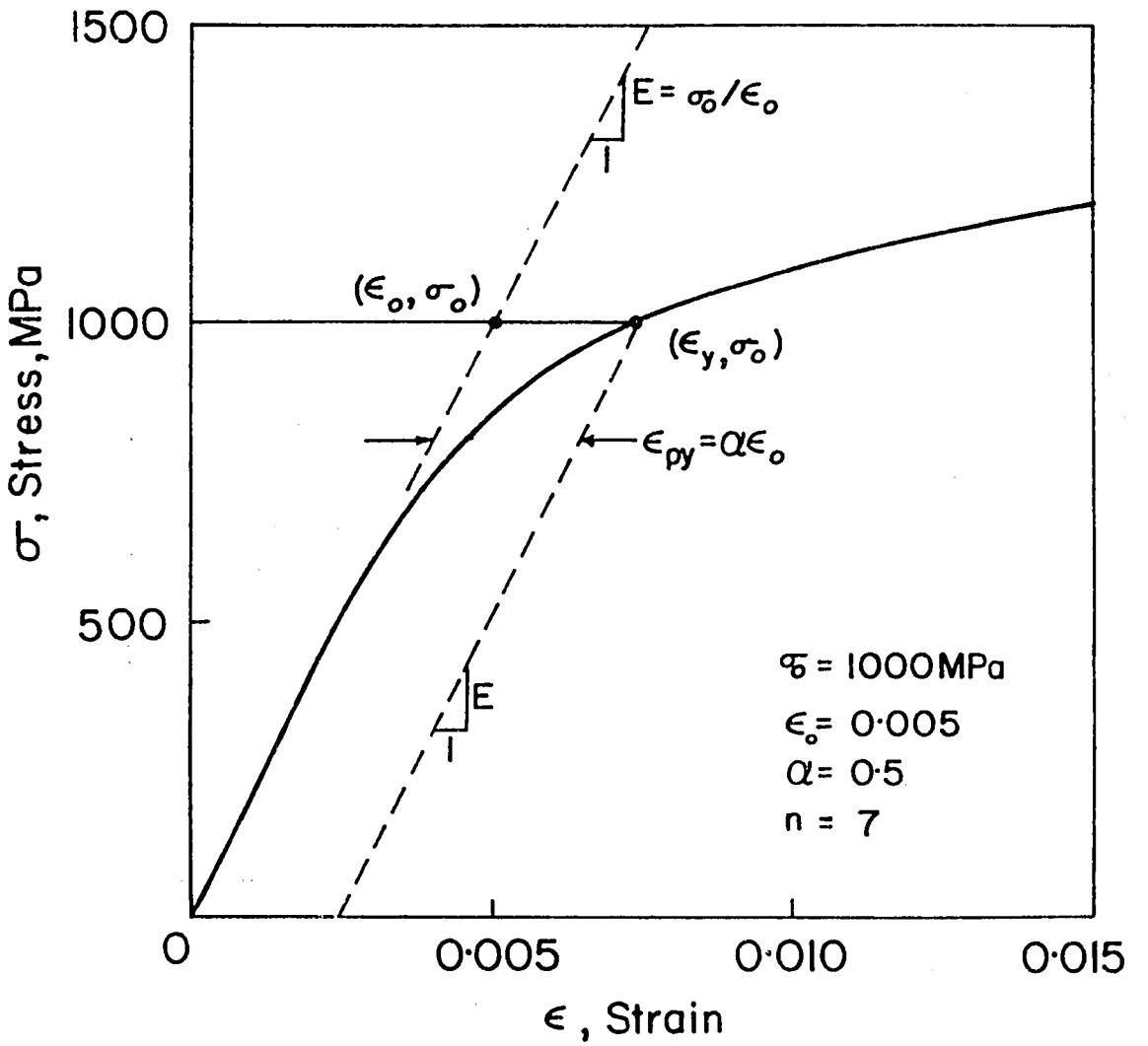

Fig. 2 - Illustration of a uniaxial stress-strain curve.

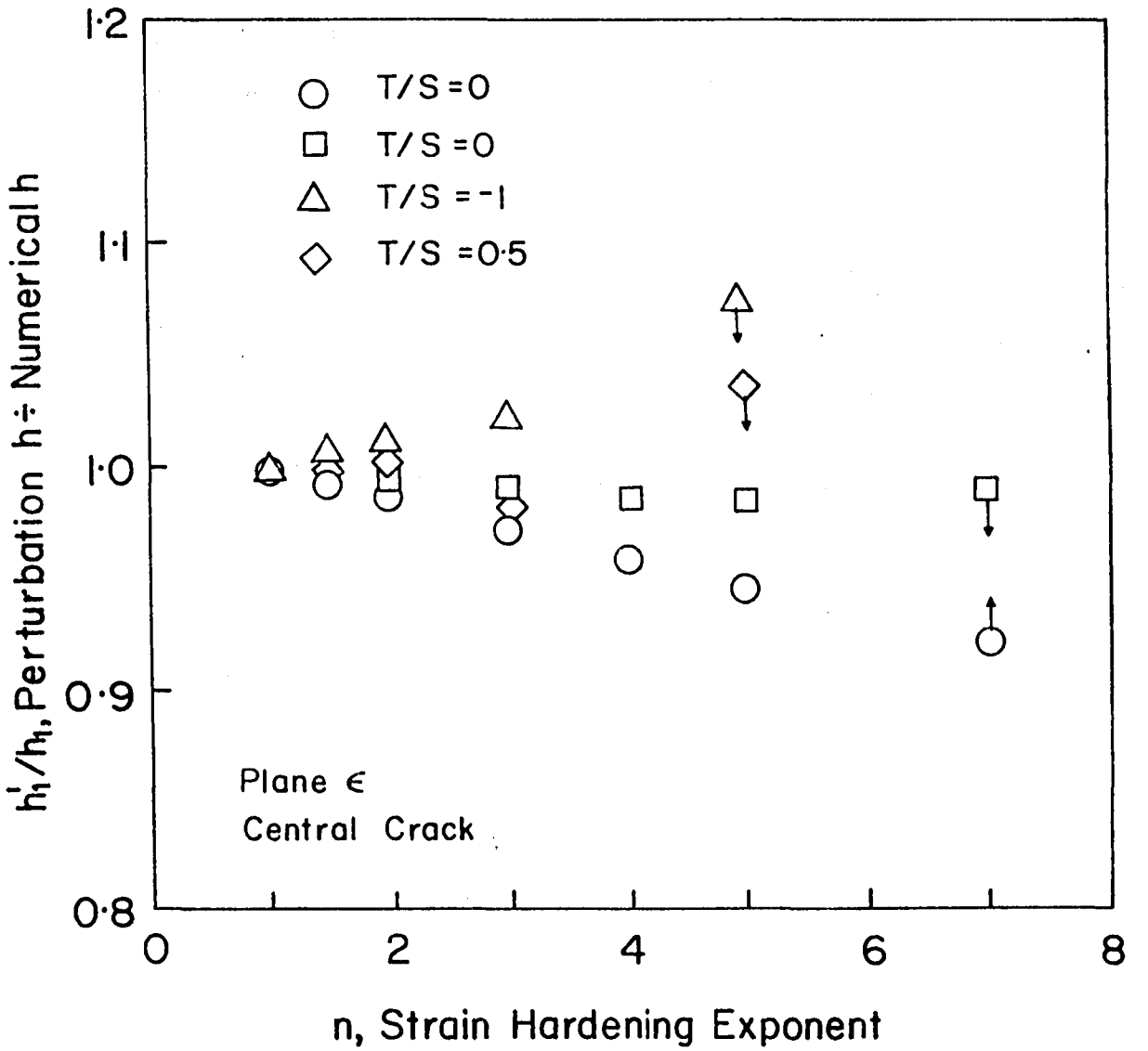

Fig. 3 - Comparison of J-integral constants from He and Hutchinson for central cracks under plane strain. The numerical h_1 values are either upper or lower bounds - see arrows.

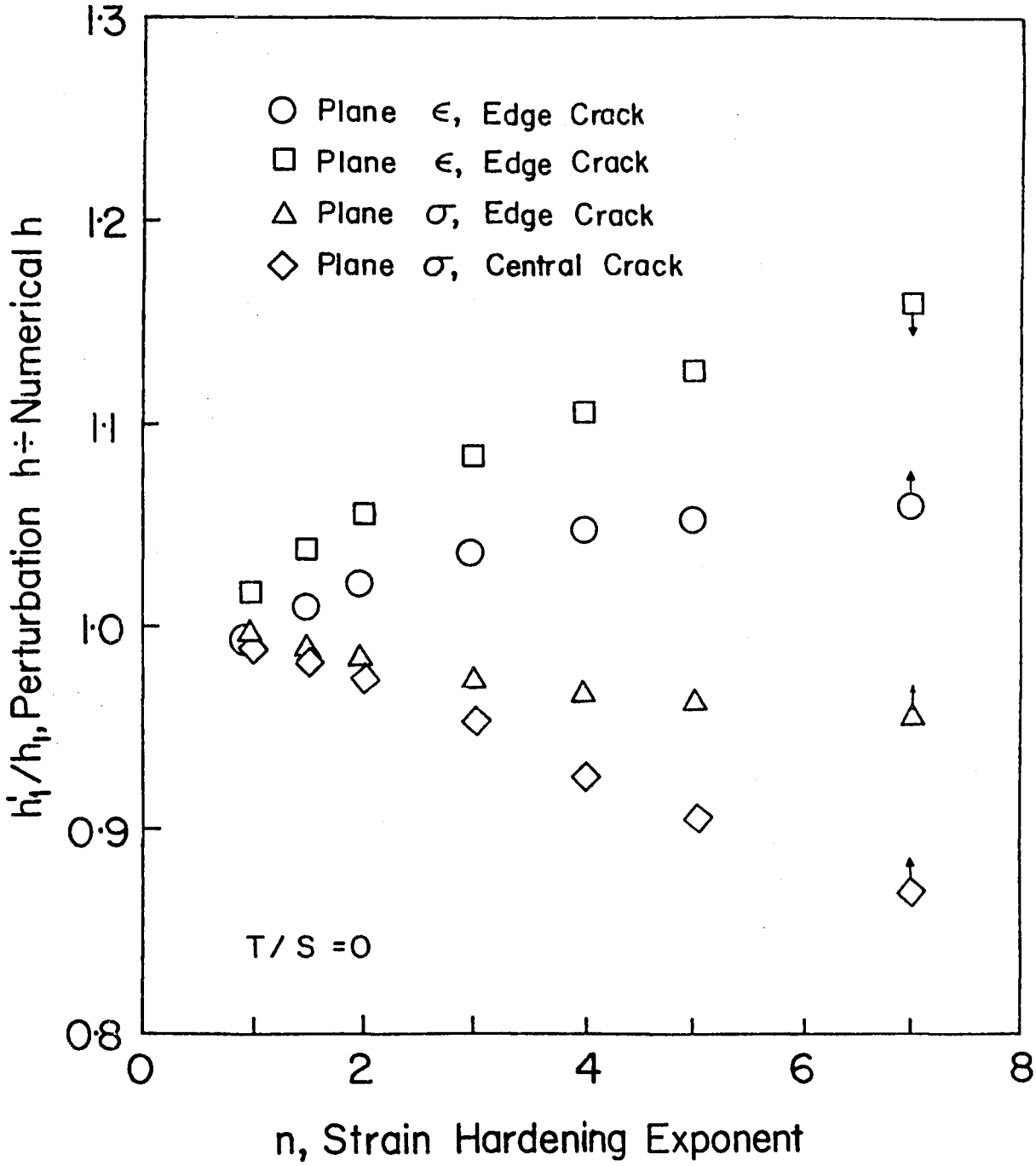

Fig. 4 - Comparison of J-integral constants from He and Hutchinson for edge cracks under plane strain, and for central and edge cracks under plane stress. The numerical h_1 values are either upper or lower bounds - see arrows.

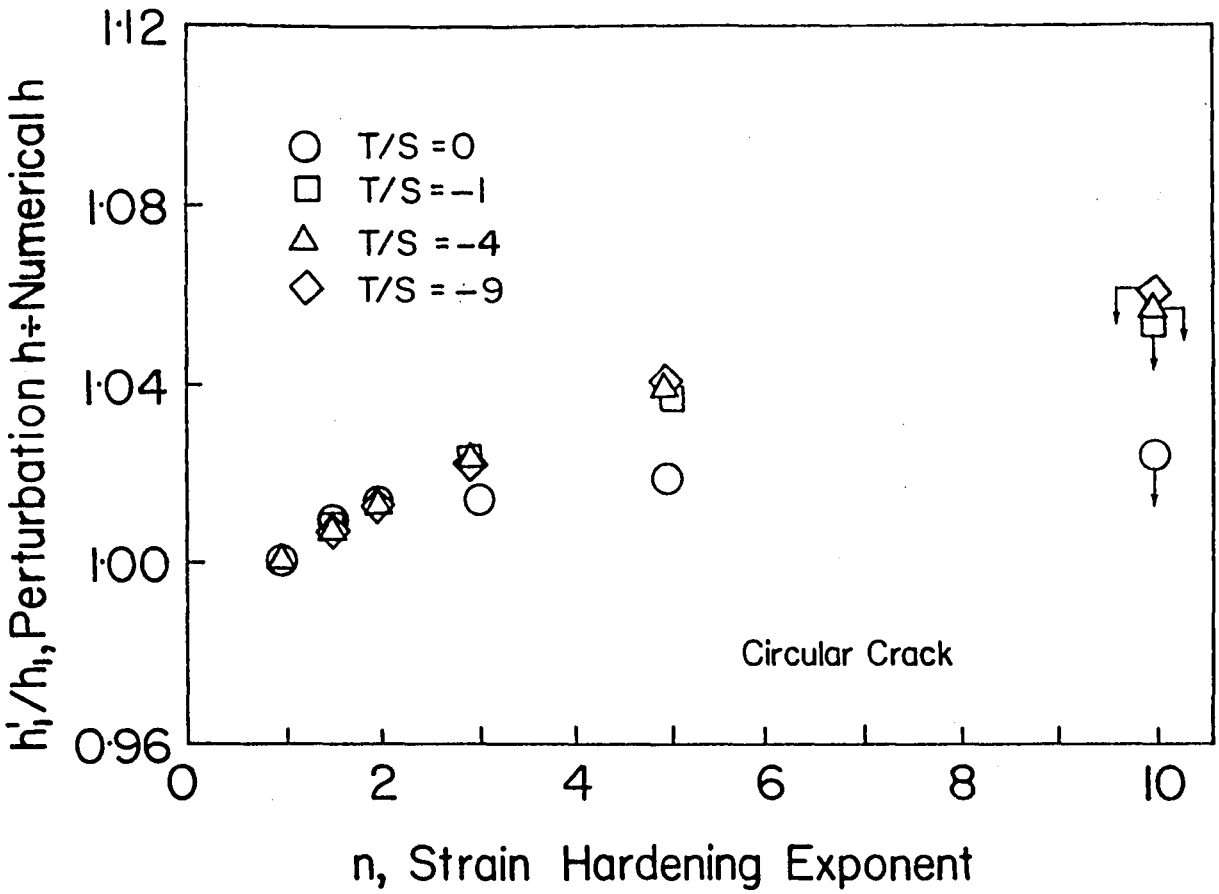

Fig. 5 - Comparison of J-integral constants from He and Hutchinson for circular cracks under axisymmetric loading, either uniaxial or with in-plane compression. The numerical h_1 values are all lower bounds - see arrows.

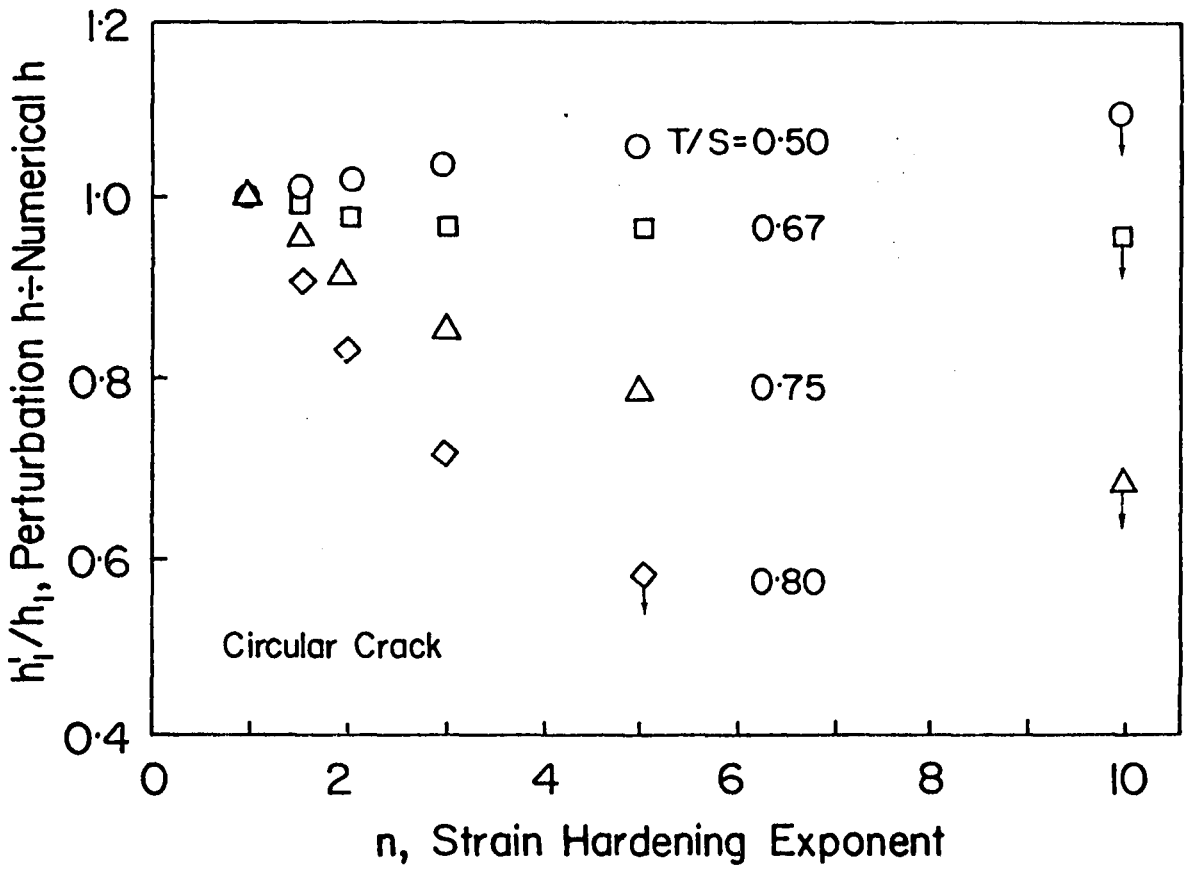

Fig. 6 - Comparison of J-integral constants from He and Hutchinson for circular cracks under axisymmetric loading with in-plane tension. The numerical h_1 values are all lower bounds - see arrows.

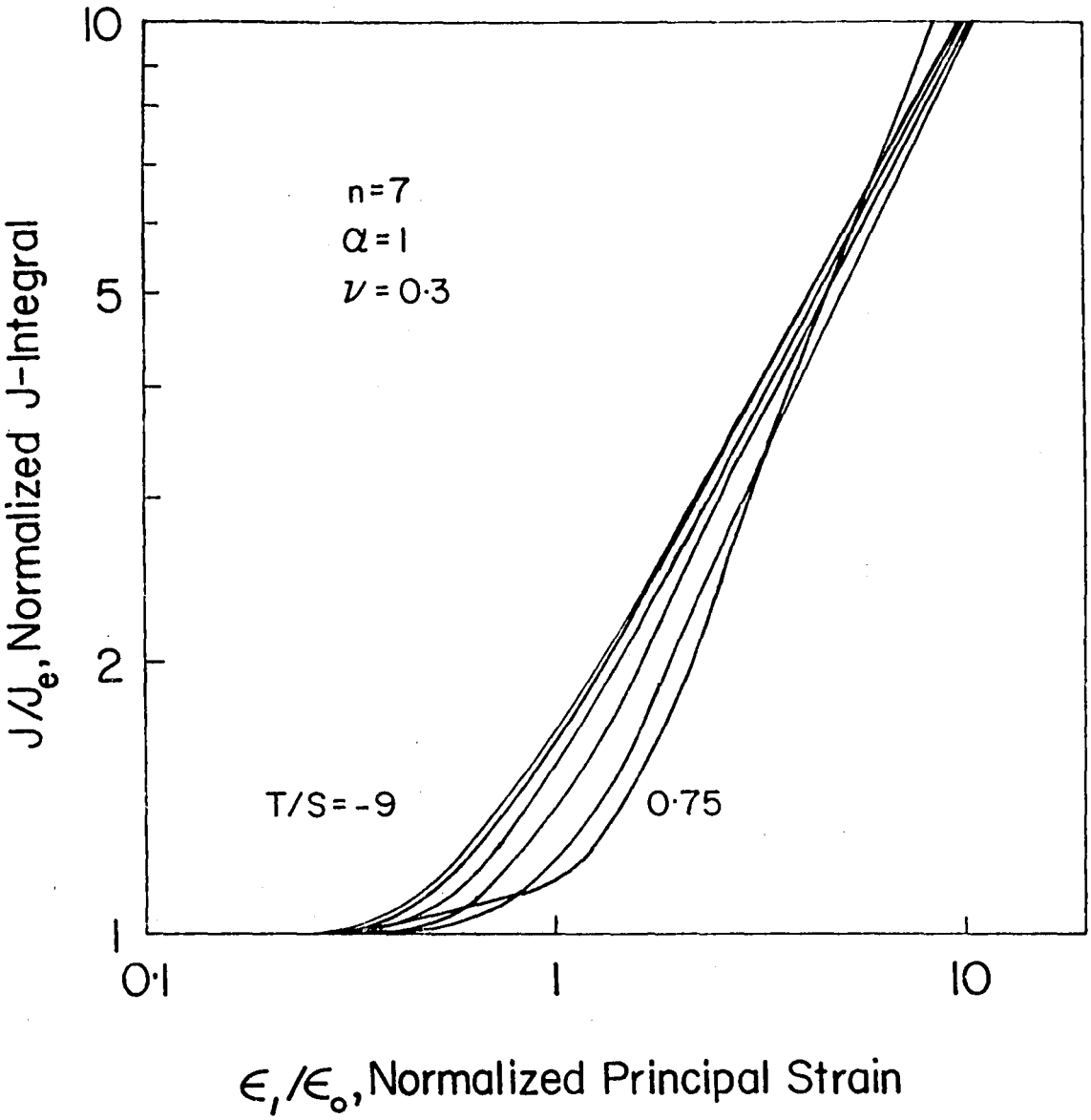

Fig. 7 - J-integral versus strain for various axisymmetric loadings applied to a circular crack.

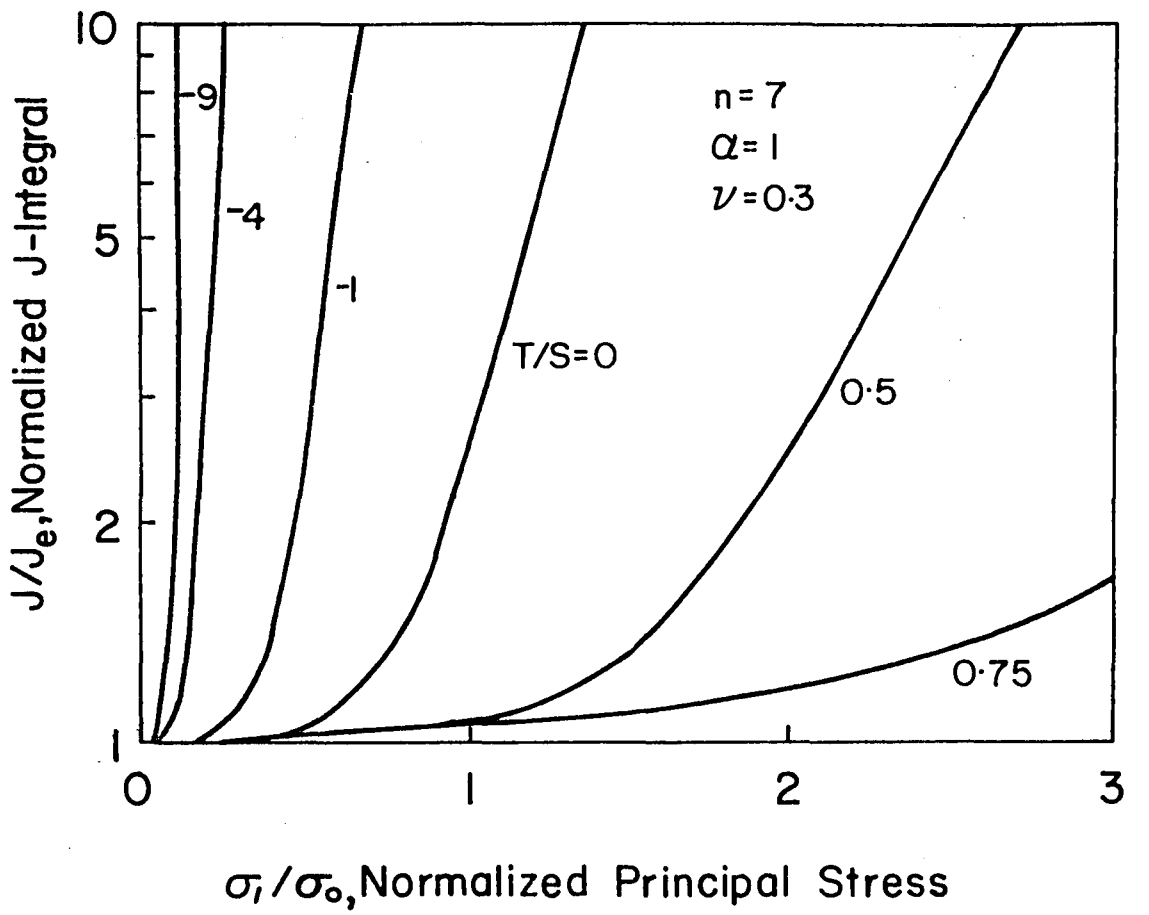

Fig. 8 - J-integral versus stress for various axisymmetric loadings applied to a circular crack.

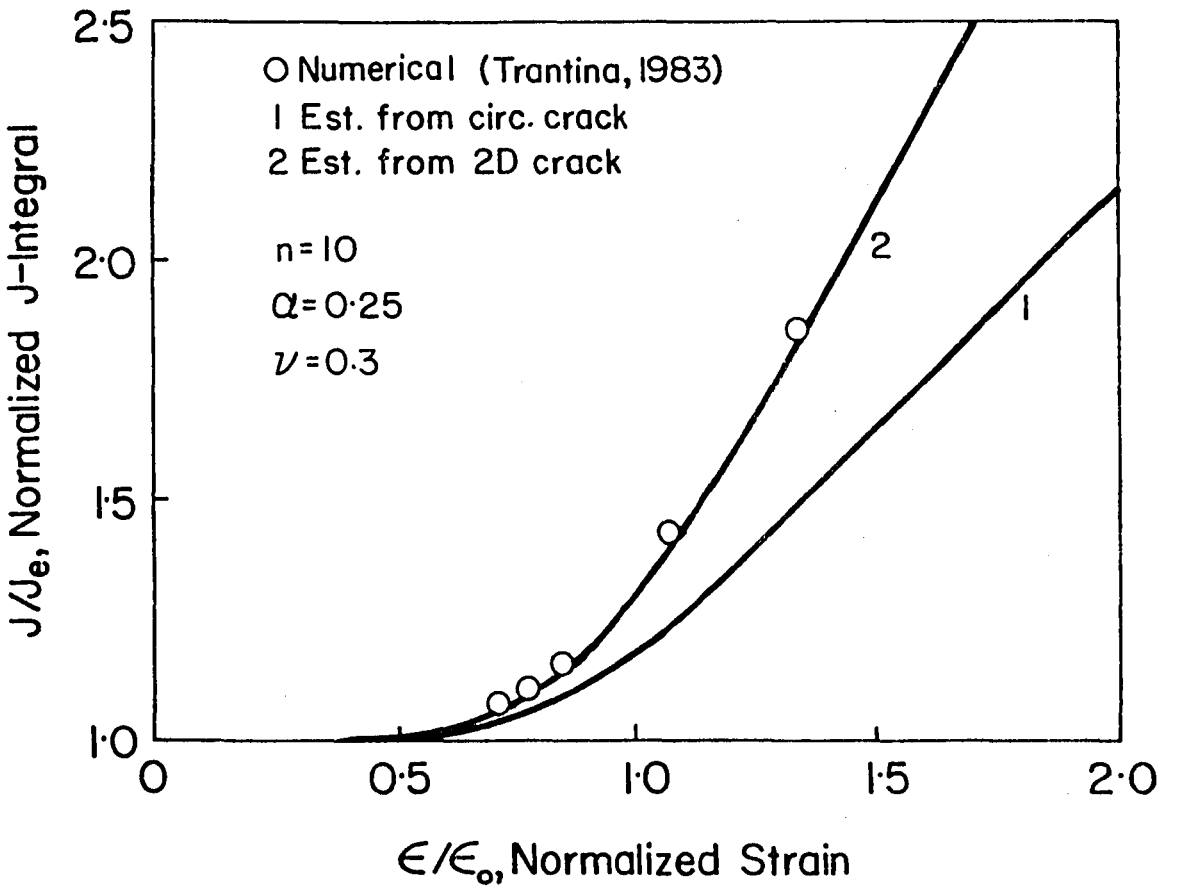

Fig. 9 - Numerical results for a half-circular surface crack under uniaxial loading compared to two estimates.

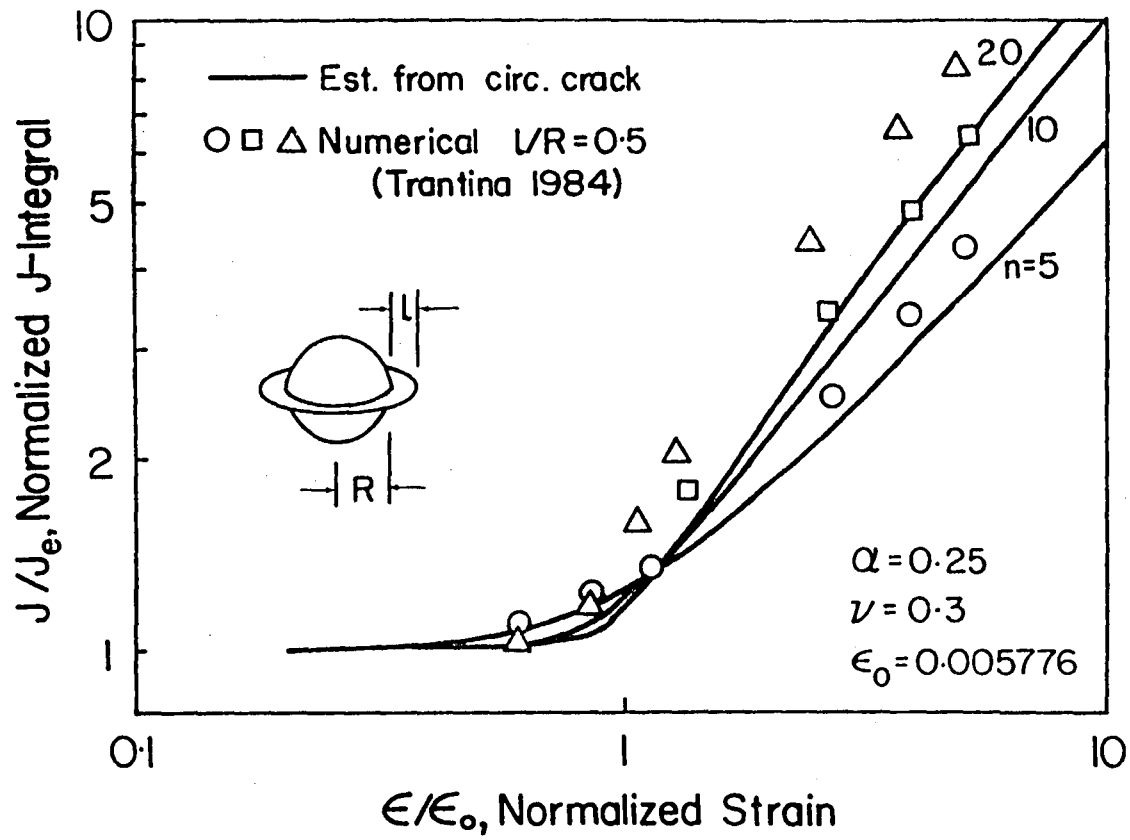

Fig. 10 - Numerical results for a circumferential crack at a spherical void under uniaxial loading compared to estimates based on a circular crack.

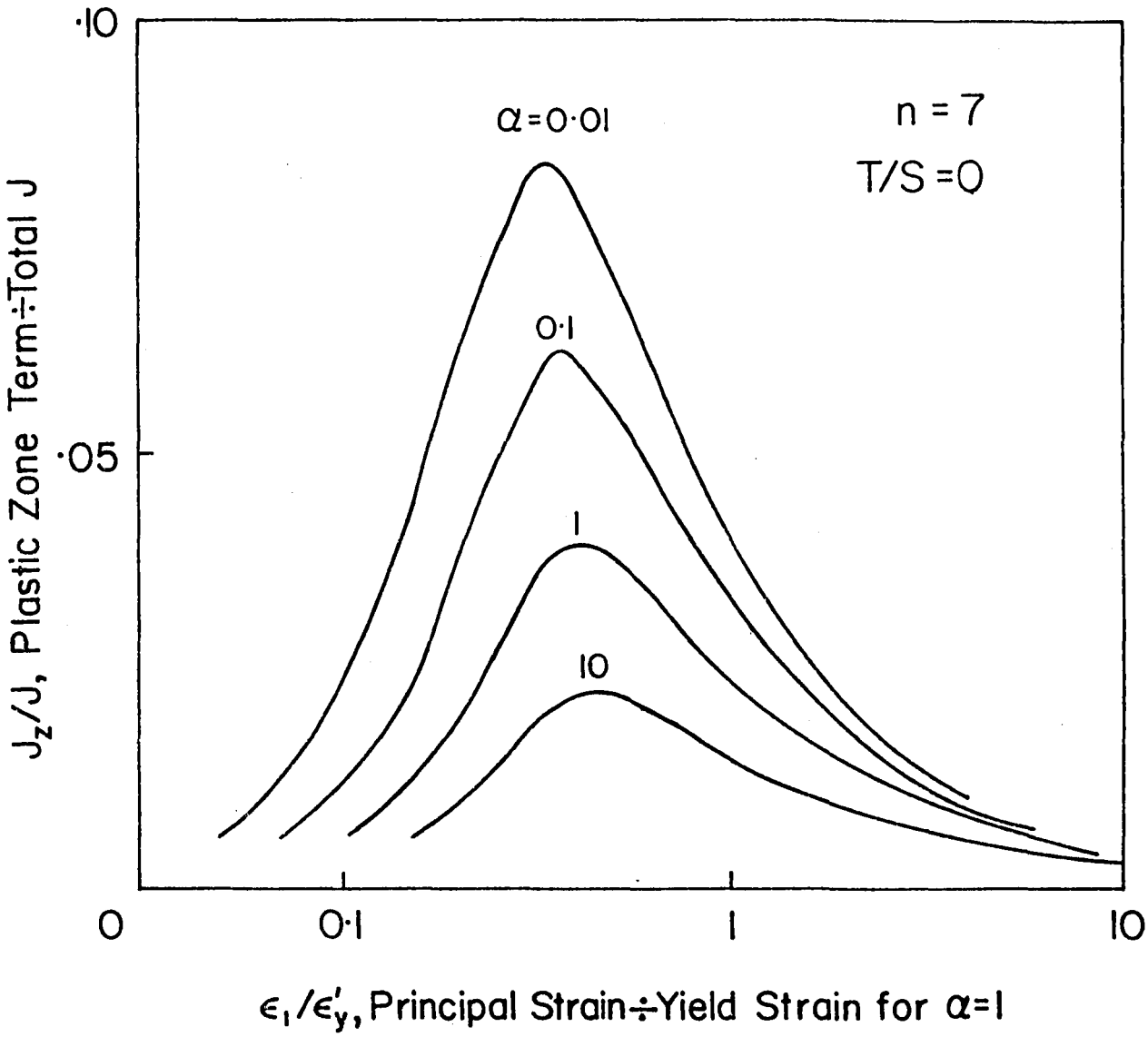

Fig. 11 - Effect of choice of α on the plastic zone correction term for an interior crack under plane strain.

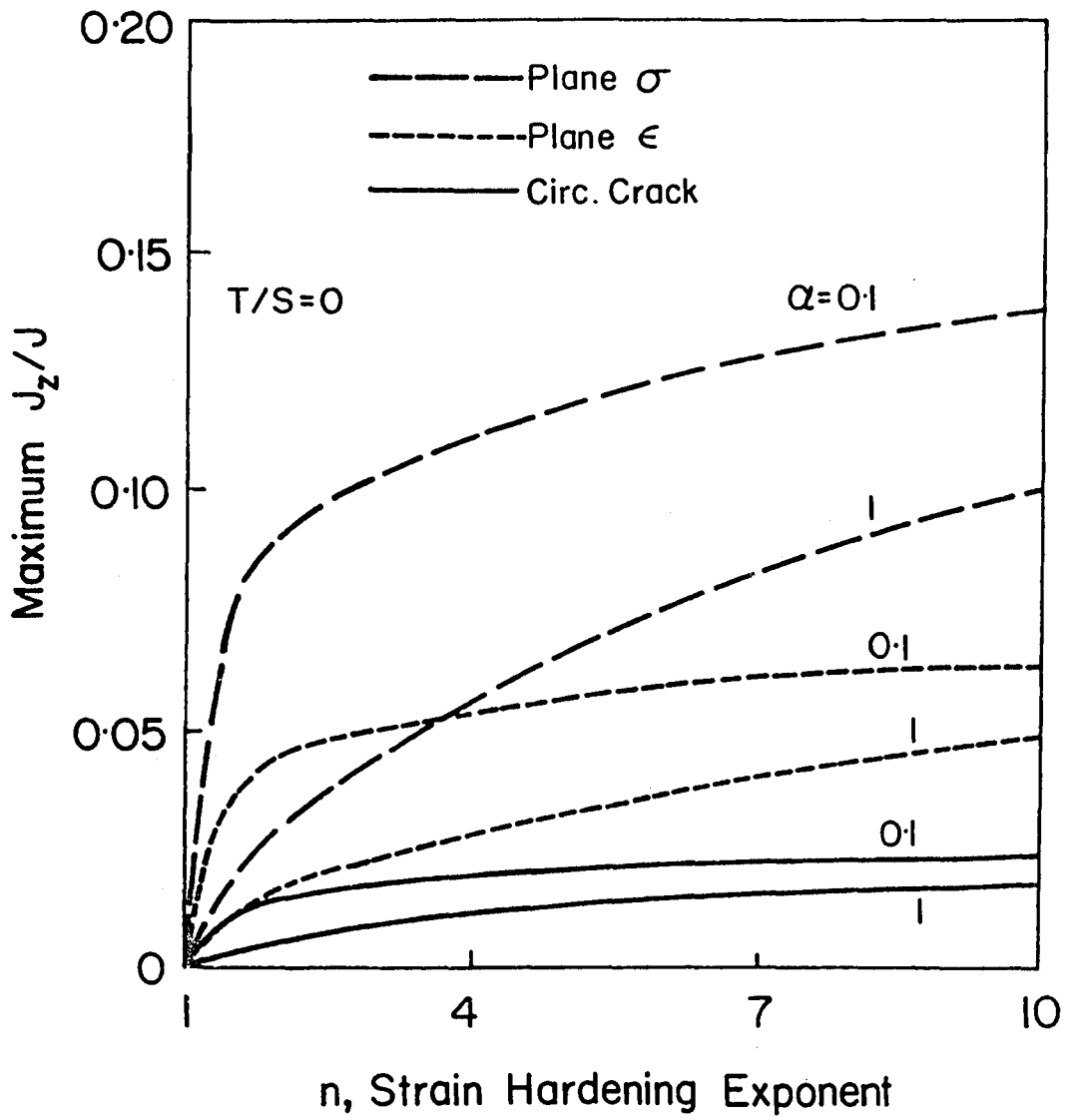

Fig. 12 - Effect of geometric constraint on the plastic zone correction term for uniaxial loading of central cracks in plane stress and plane strain and of circular cracks.

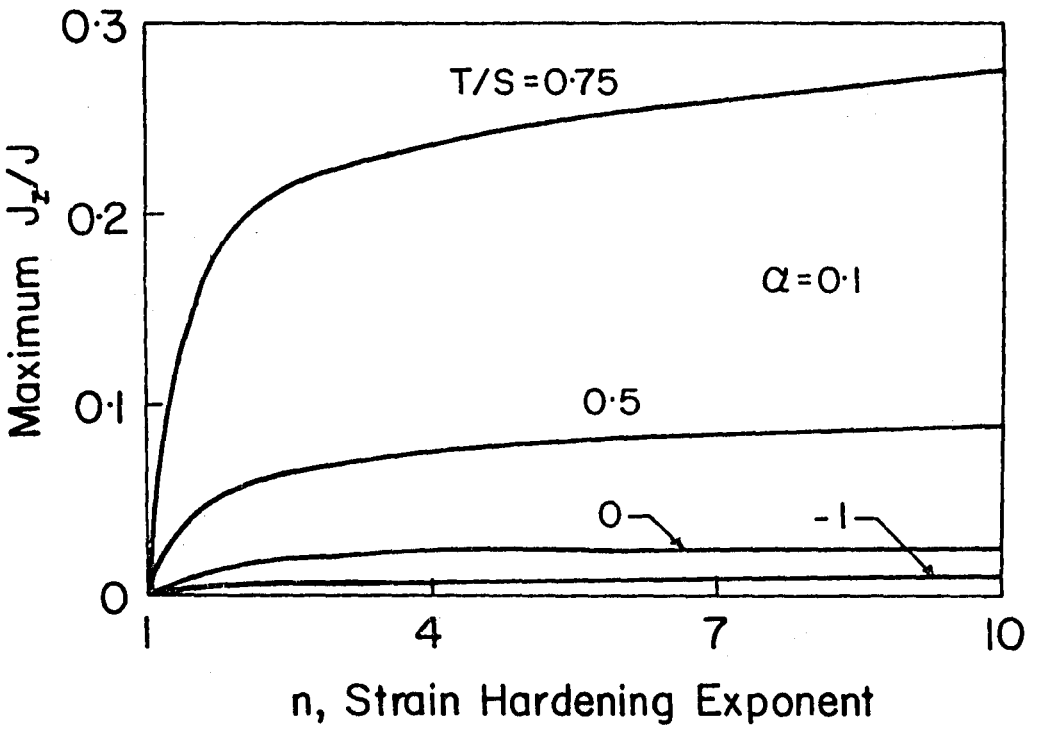

Fig. 13 - Effect of multiaxial loading on the plastic zone correction term for circular cracks under axisymmetric loading.

1. Report No.	2. Government Accession No.	3. Recipient's Catalog No.
NASA CR-179474		

4. Title and Subtitle	5. Report Date
J-Integral Estimates for Cracks in Infinite Bodies	July 1986
	6. Performing Organization Code
7. Author(s)	8. Performing Organization Report No.
N.E. Dowling	None
	10. Work Unit No.
9. Performing Organization Name and Address	11. Contract or Grant No.
Virginia Polytechnic Institute and State University Dept. of Engineering Science and Mechanics Blacksburg, Virginia 24061	NAG-3-438
	13. Type of Report and Period Covered
12. Sponsoring Agency Name and Address	Contractor Report
National Aeronautics and Space Administration Washington, D.C. 20546	14. Sponsoring Agency Code 505-63-11

15. Supplementary Notes

Final report. Project Manager, Thomas W. Orange, Structures Division, NASA Lewis Research Center, Cleveland, Ohio 44135.

16. Abstract

An analysis and discussion is presented of existing estimates of the J-integral for cracks in infinite bodies. Equations are presented which provide convenient estimates for Ramberg-Osgood type elastoplastic materials containing cracks and subjected to multiaxial loading. The relationship between J and the strain normal to the crack is noted to be only weakly dependent on state of stress. But the relationship between J and the stress normal to the crack is strongly dependent on state of stress. A plastic zone correction term often employed is found to be arbitrary, and its magnitude is seldom significant.

17. Key Words (Suggested by Author(s))	18. Distribution Statement
Crack; Plasticity; Ramberg-Osgood; Multiaxial load; J-integral	Unclassified - unlimited STAR Category 39

19. Security Classif. (of this report)	20. Security Classif. (of this page)	21. No. of pages	22. Price*
Unclassified	Unclassified	41	A03

*For sale by the National Technical Information Service, Springfield, Virginia 22161

End of Document